Available online at www.sciencedirect.com
ScienceDirect
Journal of Catalysis 251 (2007) 204–212
JOURNAL OF CATALYSIS
www.elsevier.com/locate/jcat

Silica-immobilized *N*-hydroxyphthalimide: An efficient heterogeneous autoxidation catalyst

Ive Hermans [a,*], Jeroen Van Deun [a], Kristof Houthoofd [a], Jozef Peeters [b], Pierre A. Jacobs [a]

[a] *Centre for Surface Science and Catalysis, K.U. Leuven, Kasteelpark Arenberg 23, B-3001 Heverlee, Belgium*
[b] *Department of Chemistry, K.U. Leuven, Celestijnenlaan 200F, B-3001 Heverlee, Belgium*

Received 23 May 2007; revised 21 June 2007; accepted 22 June 2007

Available online 22 August 2007

Abstract

Despite the potential of *N*-hydroxyphthalimide as a sustainable organocatalyst for autoxidations, recycling remains a largely unexplored but important topic. In this contribution, impregnation on silica is presented as a successful immobilization strategy. The activity of this catalyst during cyclohexane autoxidation is closely correlated with the support surface structure, as elucidated by ^{29}Si MAS NMR. It is found that sorption of byproducts is the main cause of deactivation such that only silicas with a low number of residual hydroxyl groups result in stable catalytic systems. Nevertheless, even for active catalysts, a slight loss in activity can be observed on a first recycling. Fortunately, the catalytic activity remains steady in subsequent recycling runs, showing only negligible additional byproduct sorption. The reduced hydroperoxide and enhanced ketone yields afforded by this catalyst is explained in terms of the phthalimide-*N*-oxyl radical chemistry, whereby this nitroxyl radical efficiently converts hydroperoxide to ketone on abstraction of the αH-atom.

Keywords: Autoxidation; Heterogeneous catalysis; Immobilization; MAS-NMR; Mechanism; NHPI; Radicals

1. Introduction

The autoxidation of hydrocarbons, such as cyclohexane, *p*-xylene, ethylbenzene, and toluene, are important processess in the chemical industry [1,2]. Yet improving the performance of such aerobic oxidations remains an industrial and scientific challenge. Recently, the radical chain chemistry was reinvestigated for two model substrates (i.e., cyclohexane and ethylbenzene) through a joint experimental and theoretical approach [3–7]. From these studies, it can be concluded that crucial reactions have been overlooked for decades. For instance, chain-carrying peroxyl radicals ($ROO^\bullet$) abstract not only H atoms from the substrate [reaction (1)], but also (even more rapidly) the weakly bonded αH-atom(s) of the hydroperoxide product (ROOH) [reaction (2)]:

$$ROO^\bullet + RH \rightarrow ROOH + R^\bullet, \tag{1}$$

$$ROO^\bullet + ROOH \rightarrow ROOH + R_{-\alpha H}{}^\bullet OOH \tag{2a}$$

$$\rightarrow ROOH + Q{=}O + {}^\bullet OH. \tag{2b}$$

This ignored propagation of the hydroperoxide is of great importance because it produces both the ketone (Q=O, where Q represents $R_{-\alpha H}$) and alcohol (ROH) products from the start of the reaction. In the past, these products were attributed to a termination reaction between two chain-carrying peroxyl radicals [1,2]:

$$ROO^\bullet + ROO^\bullet \rightarrow ROH + Q{=}O + O_2. \tag{3}$$

However, this reaction is too slow to account for a sizeable fraction of the products. Q=O originates immediately after the αH abstraction from ROOH as the $R_{-\alpha H}{}^\bullet OOH$ product radical decomposes promptly to Q=O + $^\bullet$OH [reaction (2)], thereby releasing about 30 kcal/mol [8]. The translationally "hot" $^\bullet$OH radical rapidly abstracts an H atom from a substrate molecule, surrounding the nascent products:

* Corresponding author. Fax: +32 16 321998.
E-mail address: ive.hermans@biw.kuleuven.be (I. Hermans).

0021-9517/$ – see front matter
doi:10.1016/j.jcat.2007.06.025

$$\{\mathrm{ROOH + Q{=}O + {}^{\bullet}OH}\}^{\mathrm{cage}} + \mathrm{RH}^{\mathrm{cage\text{-}wall}} \rightarrow \{\mathrm{ROOH + R^{\bullet} + Q{=}O + H_2O}\}^{\mathrm{cage}}. \quad (4)$$

This rapid abstraction reaction liberates additional heat, making the overall ROOH propagation exothermic by about 50 kcal/mol [3,4,7]. This heat causes the formation of a nanosized hot spot 200–300 K above the bulk temperature. Although the out-of-cage diffusion [reaction (5)] [9] has a lower energy barrier than the cage reaction [reaction (6)], the latter can compete because of the high temperature of the hot spot [3,4]:

$$\{\mathrm{ROOH + R^{\bullet} + Q{=}O + H_2O}\}^{\mathrm{cage}} \rightarrow \mathrm{ROOH + R^{\bullet} + Q{=}O + H_2O}, \quad (5)$$

$$\{\mathrm{ROOH + R^{\bullet} + Q{=}O + H_2O}\}^{\mathrm{cage}} \rightarrow \{\mathrm{RO^{\bullet} + ROH + Q{=}O + H_2O}\}^{\mathrm{cage}}. \quad (6)$$

Note that the cage channel [reaction (6)] causes a net destruction of ROOH and is identified as the missing alcohol source. It is important to emphasize that this revised reaction scheme readily explains the observed ol:one ratios of about 1.5 in cyclohexane oxidation and 0.5 in ethylbenzene oxidation. Indeed, the reactivity of the $R^{\bullet}$ radical governs the efficiency of the activated cage reaction [reaction (6)], rationalizing why less ROH is produced (relative to Q=O) in ethylbenzene autoxidation [7]. Whereas $RO^{\bullet}$ radicals are generally converted to additional alcohol via H abstraction from the substrate [reaction (7)], for cyclohexoxy radicals ($CyO^{\bullet}$), a unimolecular side reaction can occur [reaction (8)]:

$$\mathrm{RO^{\bullet} + RH \rightarrow ROH + R^{\bullet}}, \quad (7)$$

$$\mathrm{CyO^{\bullet} \rightarrow {}^{\bullet}CH_2{-}(CH_2)_4{-}CHO}. \quad (8)$$

During the thermal autoxidation of cyclohexane, this β-cleavage subsequent to ROOH propagation, rather than the assumed overoxidation of cyclohexanone, is responsible for most of the ring-opened byproducts [6].

An important but overlooked role of the cyclohexanone product in cyclohexane autoxidation is its assistance in the chain initiation [5]. Indeed, the efficiency of the homolytic dissociation of RO–OH [reaction (9)] is very low in the liquid phase as the nascent radicals rather recombine in their solvent-cage than they diffuse out of this Franck–Rabinowitch cage [9] and start off new chains:

$$\mathrm{ROOH \rightarrow RO^{\bullet} + {}^{\bullet}OH}. \quad (9)$$

Therefore, a pure O–O scission cannot be responsible for fast chain initiation. A new bimolecular initiation reaction between the hydroperoxide and the cyclohexanone product has been identified and kinetically quantified [5]:

$$\mathrm{CyOOH + Q{=}O \rightarrow CyO^{\bullet} + H_2O + Q_{-\alpha H}{}^{\bullet}{=}O}. \quad (10)$$

In reaction (10), the $^{\bullet}OH$ radical breaking away from the CyO–OH molecule abstracts a weakly bonded αH atom from the ketone, producing the resonance-stabilized ketonyl radical, $CyO^{\bullet}$, and water. Not only does this reaction face a lower energy barrier, also its initiation efficiency (i.e., the initiation over geminate recombination ratio) is much higher. As the ketone concentration increases sharply with time, also the initation rate increases rapidly, leading to the observed autocatalytic swing in the cyclohexane autoxidation. For substrates such as ethylbenzene, in which all C–H bonds in the ketone product are much stronger than those in cyclohexanone, the conversion increases less sharply over time compared with cyclohexane autoxidation [7]. In fact, even a slight inhibition can be observed, due to the alcohol co-oxidation ((11)–(13)), producing $HO_2^{\bullet}$ radicals [10]. These radicals terminate diffusion controlled with the chain-carrying peroxyl radicals in a head-to-tail reaction, yielding O_2 [11].

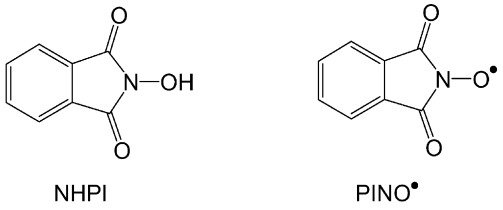

Scheme 1. Structure of *N*-hydroxyphthalimide (NHPI) and the corresponding phthalimide-*N*-oxyl radical ($PINO^{\bullet}$).

$$\mathrm{ROO^{\bullet} + ROH \rightarrow ROOH + Q^{\bullet}OH}, \quad (11)$$

$$\mathrm{Q^{\bullet}OH + O_2 \rightarrow Q(OH)OO^{\bullet}}, \quad (12)$$

and

$$\mathrm{Q(OH)OO^{\bullet} \leftrightarrows Q{=}O + HO_2^{\bullet}}. \quad (13)$$

As the chain initiation and chain termination steps together control the autoxidation rate, transition metal ions, such as $Co^{2+/3+}$ and $Mn^{2+/3+}$, often are added, because they are known to catalyze the initiation reaction [1,2]. A few years back, Ishii et al. proposed *N*-hydroxyphthalimide (NHPI, Scheme 1), with or without transition metal ions, as a homogeneous organocatalyst for the liquid-phase oxidation of several substrates [12–23]. At present, many accounts can be found on the use of various *N*-hydroxyimides as efficient catalysts for various oxyfunctionalizations [24–27]. The catalytic power of NHPI is explained by an in situ conversion to phthalimide-*N*-oxyl radicals ($PINO^{\bullet}$, Scheme 1) [26–31] on its equilibrated reaction with $ROO^{\bullet}$ radicals (14) [32,33]. $PINO^{\bullet}$ can in turn abstract H atoms from the substrate RH to regenerate NHPI and propagate the radical chain. Crucial to the catalysis is the fact that $PINO^{\bullet}$ radicals do not terminate with each other or with peroxyl radicals [32]; therefore, $PINO^{\bullet}$ is a much more efficient chain carrier than $ROO^{\bullet}$, enhancing the radical chain length. Consequently, the overall oxidation rate increases significantly. The catalytic NHPI cycle is outlined in the following reactions:

$$\mathrm{ROO^{\bullet} + NHPI \leftrightarrows ROOH + PINO^{\bullet}}, \quad (14)$$

$$\mathrm{PINO^{\bullet} + RH \rightarrow NHPI + R^{\bullet}}, \quad (15)$$

and

$$\mathrm{R^{\bullet} + O_2 \rightarrow ROO^{\bullet}}. \quad (16)$$

The catalytic efficiency (CE) of NHPI-assisted autoxidations is given by the following equation, where k^{15} and k^{1} represent the rate constants of reactions (15) and (1), respectively, and $K_{\mathrm{eq},14}$ represents the equilibrium constant of reaction (14) [32,33],

Table 1
Different silica gels used to immobilize NHPI; summary of relevant N_2-adsorption results

Silica gel	Source	BET surface[a] (m^2/g)	V^{micro}[b] (µl/g)	V^{meso}[b] (µl/g)	S^{micro}[b] (m^2/g)	S^{meso}[b] (m^2/g)
i	Redco CFT-8[c]	75	6	196	31	30
ii	Grace SP18-8506	305	8	1053	212	67
iii	Grace Si 175	558	277	0	440	0
iv	Grace SP2-8505.02	502	2	883	463	19
v	Grace Si 13/110 (13 wt% Al_2O_3)	313	2	624	98	203
vi	Grace Si–Al N°9 (0.6 wt% Al_2O_3)	500	23	1364	404	32

[a] Brunauer, Emmett, and Teller surface area.
[b] As obtained by *t*-plot analysis.
[c] See Ref. [37]; sintered at 700 °C prior to use.

$$CE = 1 + k^{15}/k^{1} \times K_{eq,14} \times [NHPI]/[ROOH]. \quad (17)$$

According to this equation, an *N*-hydroxyimide catalyst should have a fairly strong >NO–H bond to allow rapid H abstraction by the corresponding >NO• radical. If the >NO–H bond is however too weak, the corresponding nitroxyl radical becomes a radical trap. But the >NO–H bond should not be too strong, because this would shift equilibrium (14) toward the less efficient ROO• radicals. In the end, it turns out that more, but, as a consequence, slightly less reactive nitroxyl radicals result in a better catalytic performance [33].

Despite the interesting chemistry that has been developed, the cost of NHPI remains a difficult hurdle. Recycling of this organocatalyst remains an important issue to broaden the applicability of NHPI. One recycling approach that has been investigated is the covalent anchoring of NHPI to an ionic liquid [34], resulting in an interesting homogeneous process. However, heterogeneous catalysis offers several practical advantages over homogeneous catalysis [35]. To date, one heterogeneous NHPI system has been reported, unfortunately operating in acetic acid as a solvent [36].

The aim of the present work was to investigate opportunities for the design of a solvent-free heterogeneous NHPI system, based on its simple impregnation on silica. The stability and performance of these materials was studied in the autoxidation of cyclohexane and interpreted in the framework of the radical mechanism.

2. Experimental

Silica powder (Table 1) was added to a CH_3CN solution of NHPI (10 g/L) and refluxed for 12 h to disperse the catalyst throughout the support. Then the solvent was evaporated (at 130 mbar and 313 K), and the powder was dried for an additional 12 h at 343 K. The resulting material contains 0.85 mmol NHPI/g, calculated from an NHPI mass balance and confirmed by thermogravimetric analysis (TGA). The autoxidation of cyclohexane (50 ml, HPLC grade) was studied in a 100-ml stainless steel high-pressure Parr reactor, stirred at 500 rpm. Before the reactor was heated, which took about 15 min, it was pressurized with 2.76 MPa of dioxygen (99.99% purity). Prior to each experiment, the reactor was passivated with a saturated sodium pyrophosphate (pro analysis) solution, to avoid catalytic contributions from the metal wall [3]. During the reaction, the pressure was monitored continuously. The products were collected in an excess of acetone (pro analysis) and stirred for 1 h to allow desorption and dissolution of all (by)products. Subsequently, the reaction mixture was analyzed with GC-FID (50 m Cpsil-5, Chrompack column), after silylation with *N*-methyl-*N*-(trimethylsilyl)-trifluoroacetamide. Stabilizing the O–O bond and injecting at a low temperature (423 K) allowed analysis of cyclohexyl hydroperoxide. This procedure gave similar results as a method in which the hydroperoxide content was determined via the difference in alcohol content before and after reduction of the reaction mixture with trimethyl phosphine. 1-Heptanol (pro analysis) was used as an external standard. Note that autoxidation experiments are dangerous, and proper measures should be taken to protect personnel from a potential explosion.

^{29}Si MAS NMR spectra were recorded on a Bruker AMX 300. A total of 3992 scans were accumulated with a recycle delay of 60 s (at a NMR rotor spinning frequency of 5000 Hz). Infrared spectra were recorded in KBr using a Bruker IFS G6v/S spectrophotometer under 0.3 µbar vacuum (accumulation of 32 scans, 1 cm^{-1} resolution).

3. Results and discussion

3.1. Impregnation of NHPI on silica

Due to the very low solubility of NHPI in nonpolar hydrocarbons (e.g., cyclohexane) and its very large dipole moment (>4 Debye) [4], this molecule is expected to remain adsorbed on silica rather than dissolve in the liquid. Immobilization of NHPI on silica could involve not only dipole–dipole interactions, but also hydrogen bonds between silanol groups of the support and the carbonyl and >NOH groups of NHPI. Several well-characterized, off-the-shelf available silica gels, differing in surface area, pore distribution, and alumina content (Table 1), were screened. NHPI loading via impregnation was described in Section 2.

Fig. 1 compares the FTIR spectrum of an NHPI-impregnated silica gel (sample i in Table 1) with the spectra of pure NHPI and of the unloaded support. The symmetric and asymmetric carbonyl stretches of NHPI can be observed at 1790 and 1710 cm^{-1}, respectively. The broad peak at 3150 cm^{-1} corresponds to NO–H vibrations; aromatic C–H stretches are seen as a broad multiplet signal around 2900 cm^{-1}. Aromatic C–

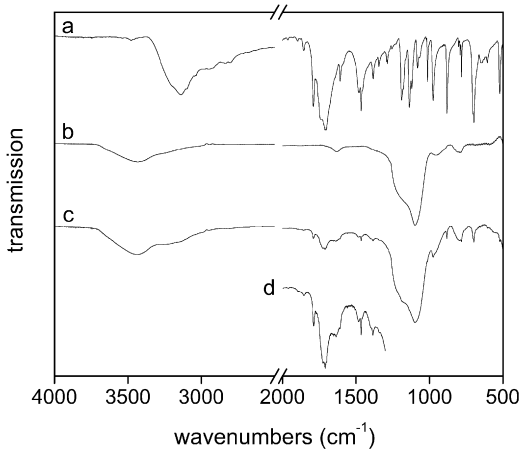

Fig. 1. FTIR spectra of NHPI (a), silica gel i (b, see Table 1) and NHPI loaded silica gel i (c); spectrum (d) is a 6×magnification of the 2000–1300 cm^{-1} range of spectrum (c).

C skeletal deformations are observed below 1610 cm^{-1}. The broad 3440 cm^{-1} peak for the SiO_2 support is a fingerprint of silanol SiO–H groups; Si–O vibrations are visible in the 1250–1000 cm^{-1} range. Nearly all NHPI vibrations can be recovered on the impregnated catalyst (spectrum c in Fig. 1). Note that despite the vacuum under which the spectra were recorded (i.e., 0.3 μbar), traces of water remained adsorbed on the silica, as evidenced by the 1650 cm^{-1} bending of water and the broad OH-stretching bands. TGA and differential scanning calorimetry (DSC) of the NHPI loaded material shows an endothermic mass loss of 1% between 300 and 425 K, due to the desorption of water. Between 425 and 960 K, DCS shows an exothermic mass loss of 14%. This value is in line with the 0.85 mmol NHPI per gram obtained from the mass balance in the impregnation step. For the pure support, no weight loss is observed in the 425–960 K range.

3.2. Catalytic screening

The six NHPI-loaded materials (supports: see Table 1) were evaluated in the 383 K autoxidation of cyclohexane (0.85 mol% NHPI or 80 mM NHPI in 50 ml CyH). At this temperature, thermal autoxidation can be neglected completely. The activity of the different samples was monitored via the O_2 consumption (Fig. 2), proportional to the alkane conversion. (The initial pressure increase is due to heating of the reactor and the establishment of the Henry equilibrium between O_2 in the gas phase and in solution.) With respect to their activity, the six powders can be divided into three different groups: active catalysts (Fig. 2a), initially active catalysts (Fig. 2b), and nonactive catalysts (Fig. 2c). A first possible explanation that came to our mind was that the active catalysts have an optimal combination of micropores and mesopores, resulting in a superior adsorption/desorption versus diffusion ratio. This hypothesis can however not explain why some silica gels featuring an analogous micropore and mesopore distribution (Table 1) show completely different catalytic behavior.

The dominant factor controlling catalytic performance can be identified from the solid-state ^{29}Si MAS NMR spectrum of

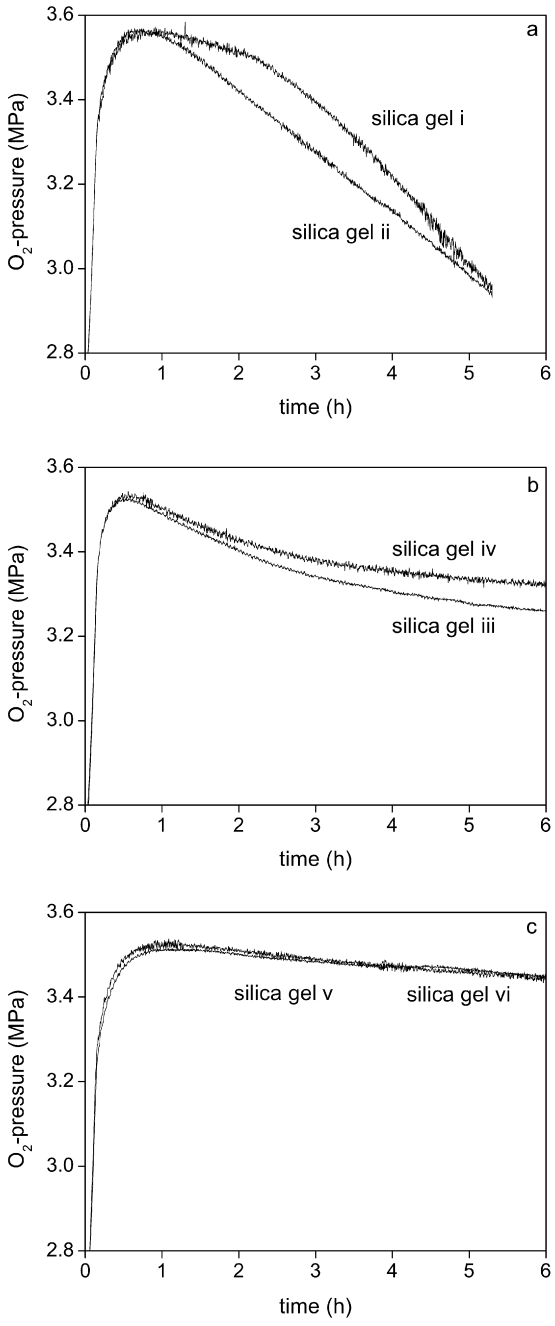

Fig. 2. O_2 consumption activity of different NHPI loaded silica gels (Table 1) in the 383 K cyclohexane autoxidation (0.85 mol% NHPI). The materials were grouped as active (a), initially active (b), and nonactive catalysts (c).

the solid supports. ^{29}Si MAS NMR is able to distinguish between Q^2 (−90 ppm), Q^3 (−100 ppm), and Q^4 (−110 ppm) Si species, containing two OH groups, one OH group, and no OH groups [bulk Si–$(OSi)_4$], respectively (see Scheme 2). Fig. 3 shows the NMR spectra for these three different catalyst categories. Clearly, the matrix has a strong influence on the catalytic performance of the system; the more polar hydroxyl groups at the surface (Q^2 or Q^3 features), the faster the catalyst tends to deactivate. The inactive catalysts also contain small quantities of alumina (see Table 1), further enhancing the polarity and acidity of the support.

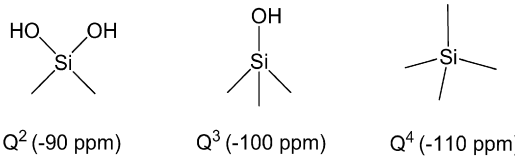

Scheme 2. Types of Si species which can be distinguished with ^{29}Si MAS NMR; between brackets are the chemical shifts.

Interestingly, the unloaded silica gels i and ii exhibited negligible catalytic activity; that is <0.1 MPa O_2 was consumed over 6 h (Fig. 4), as was also the case for pure NHPI (no oxygen consumption over 6 h). Moreover, in situ mixing of these silica gels with NHPI in the autoxidation reactor also did not result in an active system (0.1 MPa O_2 consumed over 6 h), demonstrating that the dispersion of NHPI is important in inducing a synergetic effect between the silica support and NHPI.

Fig. 5 compares the activities of the NHPI-loaded silica i and a homogeneous NHPI system (NHPI + 10 ml CH_3CN) at 403 K, both with 0.1 mol% NHPI. In this plot, the cumulative amount of consumed oxygen was derived from the recorded O_2 pressure drop during the reaction, taking into account the different gas volumes (i.e., 50 ml for the heterogeneous system and 40 ml for the homogeneous system). Apparently, the reaction rate remained more or less constant for the two systems up to 4.5% conversion, possibly due to the chain-terminating effect of $HO_2^\bullet$ radicals, counteracting (auto)catalysis. More importantly, the heterogeneous system had only slightly worse performance than the homogeneous system. This is an excellent result, taking into account that CH_3CN present in the homogeneous system acts as an initiation catalyst [38].

3.3. Stability of the catalyst

The heterogeneous nature of the catalysis was investigated under batch conditions by separating the solid catalyst from the reaction system (i.e., 0.1 mol% NHPI on silica i at 403 K). This split test (decantation) was done just below the boiling point of cyclohexane (i.e., 353 K) to avoid the readsorption of potentially leached NHPI. For the active systems, it was found that the oxidizability of the supernatant was negligible compared with that of the heterogeneous system over a period of nearly 2 h (Fig. 6). The take-off of the reaction in the supernatant after an induction period can be attributed to the presence of reaction products, including CyOOH, lighting off the thermal autoxidation. Obviously, if the observed activity in the heterogeneous system was due to leached NHPI, then the O_2 consumption rate would remain identical in the supernatants. These findings are consistent with the negligible amount of NHPI detected in the liquid phase by GC (i.e., 3 mM, or <4% of the immobilized NHPI) after 4 h of reaction. Presumably, this small fraction of leaching stems from the few NHPI molecules weakly sorbed to the silica.

On the other hand, it was found that the activity of the recycled catalyst was significantly lower than that of the fresh catalyst (Fig. 7). However, the activity remained steady after this initial activity loss in the first recycle. This transient behavior is most likely caused by the sorption of reaction products,

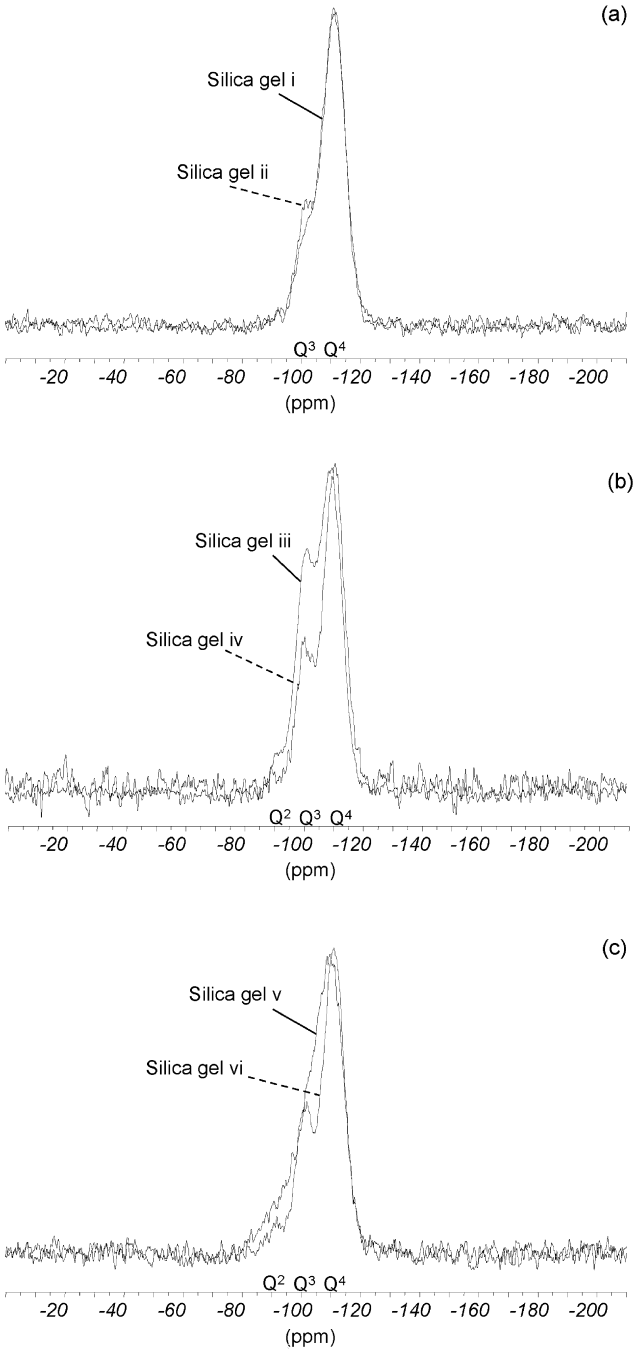

Fig. 3. ^{29}Si MAS NMR spectra of the silica supports (Table 1), grouped according to the observed autoxidation activity in Fig. 2.

in particular ring-opened byproducts such as adipic acid, because leaching of NHPI can be neglected (vide supra). Sorption of adipic acid indeed could involve chelating H bonds, causing screening/blocking of the active NHPI sites. In addition, an increased mass loss can be observed with TGA, consistent with the sorption hypothesis. Apparently, the (most) favorable silanol sites are already occupied by (by)products during the first catalytic run, and no further deactivation occurs as the smaller energy decrease on sorption to the remaining sites no longer balances the entropy loss. Fig. 8 shows the FTIR spectrum of the catalyst as a function of the reaction time. A clear

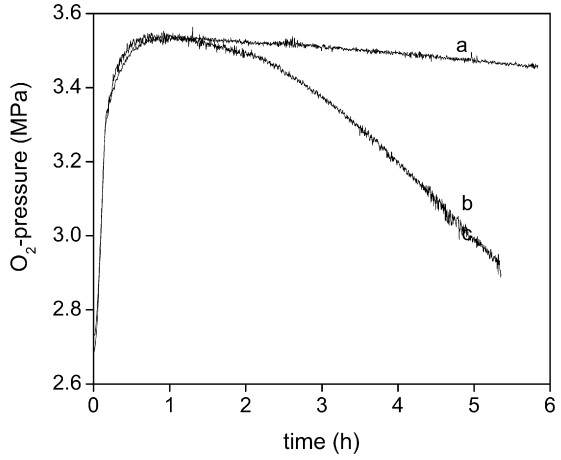

Fig. 4. O_2 consumption activity of silica gel i (a) and NHPI loaded silica gel i (b, 0.85 mol% NHPI) in the 383 K autoxidation of cyclohexane.

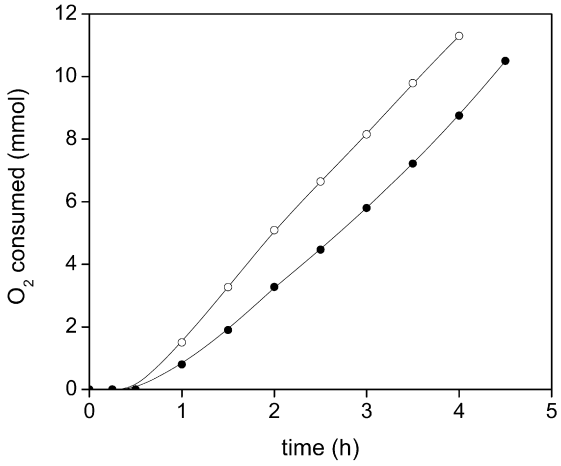

Fig. 5. Consumed O_2 in the 403 K autoxidation of 50 ml cyclohexane, catalyzed by 0.1 mol% NHPI, homogeneous ((○) plus 10 ml CH_3CN) and heterogeneous ((●) 0.85 mmol NHPI per gram silica gel i).

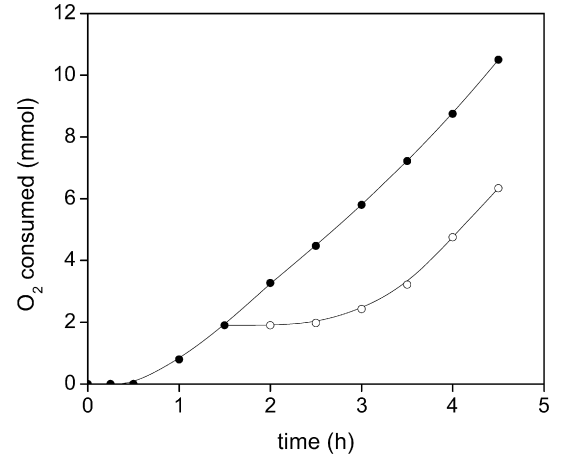

Fig. 6. Cumulative amount of O_2 consumed during the 403 K cyclohexane autoxidation, catalyzed by 0.1 mol% of the heterogeneous NHPI loaded silica gel i (solid symbols) and during the subsequent oxidation of the supernatant, separated from the solid catalyst after 1.5 h (open symbols).

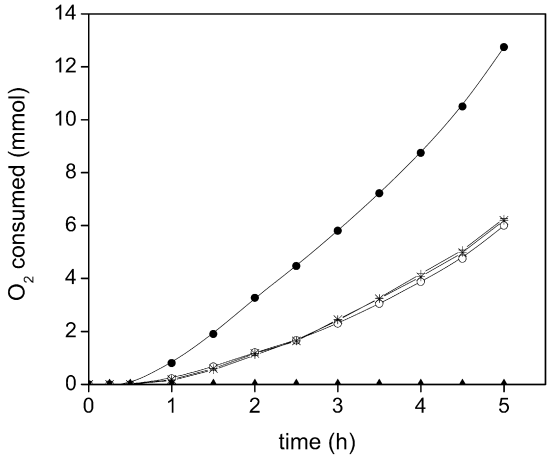

Fig. 7. Comparison of the 403 K cyclohexane autoxidation activity of a fresh heterogeneous NHPI loaded silica gel i (solid symbols, 0.1 mol% NHPI) and recycled catalysts after 6 mmol O_2 has been consumed (first recycle (○), second recycle (∗), third recycle (+)).

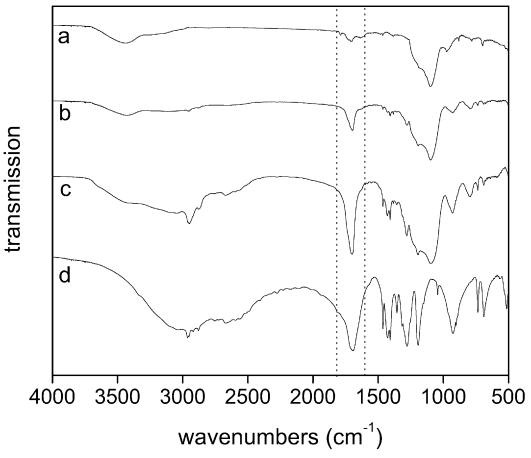

Fig. 8. FTIR spectra of the fresh NHPI-loaded silica gel i (a), after 2 (b) and 5 h (c) of cyclohexane autoxidation at 403 K, compared with the spectrum of adipic acid (d).

broadening of the C=O stretching region (1650–1950 cm^{-1}) can be observed, associated with the appearance of C–H vibrations (2800–3000 cm^{-1}) arising from aliphatic compounds. Comparing these spectra with the spectrum of adipic acid in Fig. 8 identifies this compound as the catalyst poison.

From these results, it must be concluded that the observed activity is due to true heterogeneous catalysis. On recycling, the catalyst first goes through a transient regime and then acquires steady activity, due to a balanced sorption of adipic acid. This system not only is interesting from a practical standpoint, but also can be used to study the effect of nitroxyl radical (i.e., PINO•) propagation on product makeup without the influence of a solvent as in earlier homogeneous systems [4].

3.4. Performance of the heterogeneous catalyst

The product distribution from cyclohexane autoxidation at 403 K in the presence of the active catalysts (i.e., NHPI-loaded silica gels i and ii) is very similar. Fig. 9 compares the performance of sample i (0.1 mol% NHPI) with thermal autoxidation

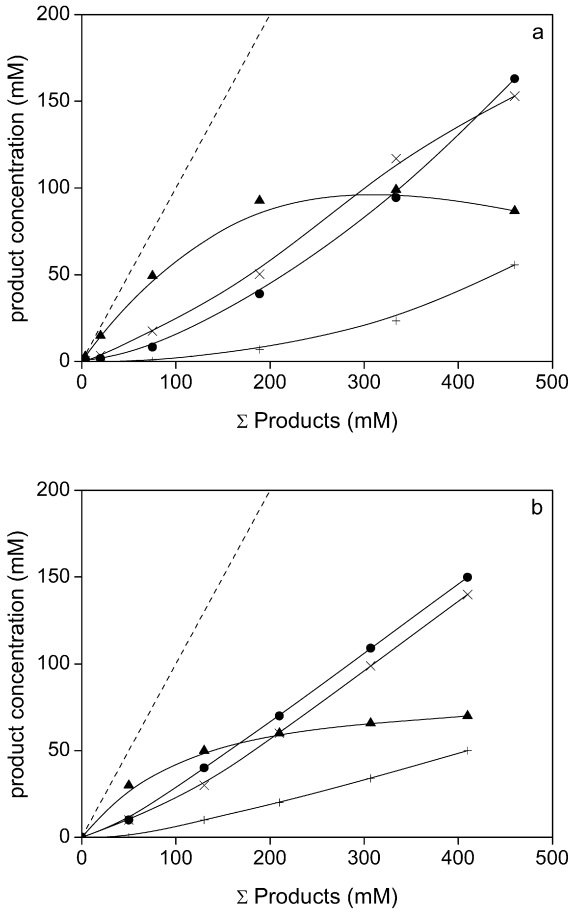

Fig. 9. Product distribution at 403 K during the pure thermal cyclohexane autoxidation (a), and upon addition of the immobilized NHPI catalyst (b, 0.1 mol% of NHPI on silica gel i). ((▲) CyOOH, (×) CyOH, (●) Q=O, (+) by-products.)

in the relevant 0–5% conversion range. It is important to emphasize that the GC-based conversion is in line with the O_2 consumption; that is, similar GC conversions were obtained for the same amount of O_2 consumed in the heterogeneous and homogeneous systems. This ensures that all (by)products were collected and analyzed properly in our analytical procedure (see Section 2). At 403 K, it took the thermal system more than 20 h to achieve a conversion of 4.5%, whereas in the presence of the immobilized NHPI catalyst i at just 0.1 mol%, the time scale of the reaction was reduced to about 5 h.

A striking observation is that on addition of the heterogeneous NHPI catalyst, the hydroperoxide yield was reduced by about a factor of two. This finding can be ascribed to the involvement of PINO$^\bullet$ radicals. Nevertheless, CyOOH remained the (exclusive) primary reaction product, as demonstrated by the initial finite slope and negative second derivative of its contribution in Fig. 9b. As emphasized in Section 1, αH abstraction from hydroperoxide is a very important reaction in determining the product distribution. Therefore, the reactivity of PINO$^\bullet$ toward CyOOH should be evaluated. Based on the previously computed energy barriers of reactions (19) and (2) (i.e., 8.2 and 11.8 kcal/mol, respectively), we can estimate that free PINO$^\bullet$ radicals react about 25 times faster with CyOOH than CyOO$^\bullet$ radicals. This estimation takes approximately into account the more rigid character of the transition state of reaction (19) compared with reaction (2), due to a stronger H bond between the two species. Not only does PINO$^\bullet$ react faster with the hydroperoxide product, reaction (19) also causes a stoechiometric destruction of CyOOH, thereby reducing the hydroperoxide yield even more:

$$\text{PINO}^\bullet + \text{CyH} \rightarrow \text{NHPI} + \text{Cy}^\bullet, \tag{18}$$

$$\text{PINO}^\bullet + \text{CyOOH} \rightarrow \text{NHPI} + \text{Q=O} + {}^\bullet\text{OH}. \tag{19}$$

It is indeed important to emphasize that an efficient cage reaction such as (6) cannot occur subsequent to (19). This rationalizes the reversed ol:one ratio, because CyOOH propagation by PINO$^\bullet$ yields only Q=O and no CyOH. Alcohol arises only from CyOOH propagation by CyOO$^\bullet$ radicals, according to reaction (6). From the measured ol/one ratios in the thermal and NHPI catalyzed reactions (viz. 1.5 and 0.75, respectively at 1.7% conversion), one can estimate PINO$^\bullet$/CyOO$^\bullet$ $\approx$ 0.04,[1] taking into account that PINO$^\bullet$ reacts 25 times faster with CyOOH compared with CyOO$^\bullet$(vide supra). Combining this estimated value with [ROOH] = 50 mM and [NHPI] = 9.3 mM, one can compute $K_{\text{eq},14} \approx 0.2$. Given the expected error of a factor of 50,[2] this value is in line with the theoretically predicated O–H bond strengths in NHPI and ROOH[3] [33]. Thus, it appears that only a very small fraction of the chain propagators are PINO$^\bullet$ radicals, explaining why the CyOOH yield decreased by only a factor of two compared with the thermal system. The ability of such a small amount of PINO$^\bullet$ to induce a significant catalytic effect can be attributed to its intrinsically higher reactivity. For instance, PINO$^\bullet$ radicals react about 7 times faster with CyH [reaction (18)] than CyOO$^\bullet$ radicals, as predicted by the computed energy barriers of 16.0 and 17.6 kcal/mol, respectively [3,33].

The decreased importance of the activated cage reaction (6) is also reflected by the evolution of (ring-opened) byproducts in Fig. 10. During the pure thermal autoxidation, 6-hydroxyhexanoic acid was identified as the exclusive primary byproduct from which nearly all other byproducts were subsequently formed [6]. 6-Hydroxyhexanoic acid was demonstrated to originate from CyO$^\bullet$ radicals through reaction (8) and the subsequent ω-formyl chemistry. In the present system, less CyO$^\bullet$ radicals are produced in CyOOH propagation, as reflected by the evolution of 6-hydroxyhexanoic acid shown in Fig. 9; this compound is no longer the exclusive primary byproduct. Adipic acid clearly appears as a primary byproduct rather than a secondary one. This implies that the dominant mechanism for byproduct formation differs from that for the pure thermal autoxidation system. Most likely, αH abstraction from the cyclohexanone product, relative to the alkane

[1] The propagation of CyOOH by CyOO$^\bullet$ produces 1.5 CyOH and 1 Q=O whereas the propagation by PINO$^\bullet$ only produces 1 Q=O; so for a PINO$^\bullet$/CyOO$^\bullet$ ratio of 0.04/0.96, the expected ol/one ratio equals $0.96 \times 1.5/(25 \times 0.04 + 0.96) = 0.7$; the factor 25 in the denominator stems from the reactivity ratio of PINO$^\bullet$ vs CyOO$^\bullet$ toward CyOOH.

[2] This error is caused, among others, by the uncertainty on the reactivity of immobilized PINO$^\bullet$ radicals toward CyOOH, and by ignoring the co-oxidation of CyOH when determining the ol:one ratio.

[3] $\Delta_r E$ of reaction (14) could be influenced by the silica support.

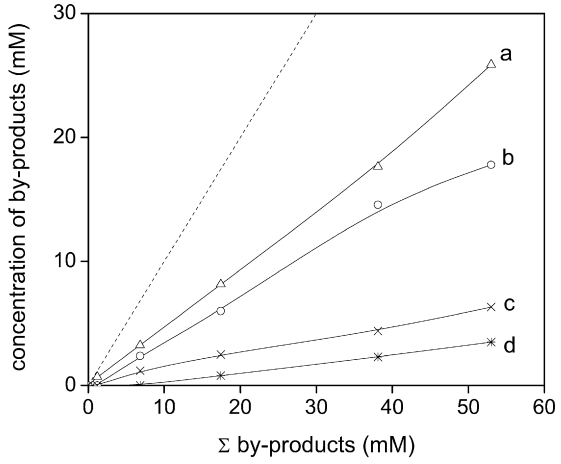

Fig. 10. Evolution of the by-products as a function of their sum. Adipic acid (a), 6-hydroxyhexanoic acid (b), ε-caprolactone (c), and glutaric acid (d).

substrate, is faster by PINO$^\bullet$ radicals than by ROO$^\bullet$ radicals. Indeed, based on the computed barriers for αH abstraction from CyH and Q=O by PINO$^\bullet$ (16.0 and 13.5 kcal/mol, respectively) [4], the estimated k(Q=O)/k(CyH) rate constant ratio was ≈10. In comparison, this ratio was 5 for CyOO$^\bullet$ radicals, explaining, in combination with a significantly higher Q=O yield, the observed evolution of byproducts shown in Fig. 10 (although the precise mechanism remains under investigation).

It also should be mentioned that the product distribution obtained with a recycled catalyst was very similar to that for a fresh catalyst; for example, with a catalyst recycled after 3 h, the product makeup after 5 h of reaction with pure cyclohexane was 85.1 mM of Q=O, 66.2 of CyOH, 53.5 of CyOOH, and 29.1 of byproducts. So, for a sum of products equal to 234.0 mM, this product distribution resembles that obtained with a fresh catalyst (Fig. 9b).

4. Conclusion

This study on *N*-hydroxyphthalimide immobilization demonstrates the potential for designing active and stable heterogeneous catalytic systems via impregnation on silica. A close correlation between the surface structure of the support and the catalyst activity was observed. With a high surface density of silanol groups, ring-opened byproducts, such as adipic acid, stick to the surface of the catalyst so as to screen off the active NHPI sites. This sorption effect even puts its mark on active catalysts with few silanol groups, because it causes a slight loss in activity on recycling of the material. Fortunately, the byproduct sorption soon attains a steady level, leading to stable activity after a first recycling. The immobilized catalyst results in a favorable product distribution with a reduced hydroperoxide yield and an increased ketone yield. This is the result of the propagating action of phthalimide-*N*-oxyl radicals, reacting much faster than peroxyl radicals with the hydroperoxide product. This abstraction reaction causes net consumption of the hydroperoxide and simultaneous formation of the desired ketone.

Acknowledgments

This work was performed under the GOA (KU Leuven), CECAT (KU Leuven), and IDECAT (EC) projects and the Belgian Program on Interuniversity Attraction Poles (IAP). I.H. is indebted to FWO-Vlaanderen for a research position.

References

[1] R.A. Sheldon, J.K. Kochi, Metal-Catalyzed Oxidations of Organic Compounds, Academic Press, New York, 1981.
[2] G. Franz, R.A. Sheldon, Oxidation, Ullmann's Encyclopedia of Industrial Chemistry, Wiley–VCH, Weinheim, 2000.
[3] I. Hermans, T.L. Nguyen, P.A. Jacobs, J. Peeters, Chem. Phys. Chem. 6 (2005) 637.
[4] I. Hermans, P.A. Jacobs, J. Peeters, J. Mol. Catal. A Chem. 251 (2006) 221.
[5] I. Hermans, P.A. Jacobs, J. Peeters, Chem. Eur. J. 12 (2006) 4229.
[6] I. Hermans, P.A. Jacobs, J. Peeters, Chem. Eur. J. 13 (2007) 754.
[7] I. Hermans, J. Peeters, P. Jacobs, J. Org. Chem. 72 (2007) 3057.
[8] L. Vereecken, T.L. Nguyen, I. Hermans, J. Peeters, Chem. Phys. Lett. 393 (2004) 432.
[9] S.W. Benson, The Foundations of Chemical Kinetics, McGraw–Hill, New York, 1960.
[10] I. Hermans, J.-F. Müller, T.L. Nguyen, P.A. Jacobs, J. Peeters, J. Phys. Chem. A 109 (2005) 4303.
[11] D.M. Rowley, R. Lesclaux, P.D. Lightfoot, B. Nozière, T.J. Wallington, M.D. Hurley, J. Phys. Chem. 96 (1992) 4889.
[12] Y. Ishii, K. Nakayama, M. Takeno, S. Sakaguchi, T. Iwahama, Y. Nishiyama, J. Org. Chem. 60 (13) (1995) 3934.
[13] T. Iwahama, S. Sakaguchi, Y. Nishiyama, Y. Ishii, Tetrahedron 36 (38) (1995) 6923.
[14] Y. Ishii, T. Iwahama, S. Sakaguchi, K. Nakayama, Y. Nishiyama, J. Org. Chem. 61 (14) (1996) 4520.
[15] Y. Ishii, S. Kato, T. Iwahama, S. Sakaguchi, Tetrahedron Lett. 37 (28) (1996) 4993.
[16] Y. Ishii, J. Mol. Catal. A Chem. 117 (1–3) (1997) 123.
[17] Y. Yoshino, Y. Hayashi, T. Iwahama, S. Sakaguchi, Y. Ishii, J. Org. Chem. 62 (20) (1997) 6810.
[18] S. Kato, T. Iwahama, S. Sakaguchi, Y. Ishii, J. Org. Chem. 63 (2) (1998) 222.
[19] T. Iwahama, K. Syojyo, S. Sakaguchi, Y. Ishii, Org. Proc. Res. Dev. 2 (4) (1998) 255.
[20] S. Sakaguchi, T. Takase, T. Iwahama, Y. Ishii, Chem. Commun. 18 (1998) 2037.
[21] T. Iwahama, S. Sakaguchi, Y. Ishii, Tetrahedron Lett. 39 (49) (1998) 9059.
[22] Y. Ishii, S. Sakaguchi, Catal. Surv. Jpn. 3 (1999) 27.
[23] T. Iwahama, S. Sakaguchi, Y. Ishii, Chem. Commun. 7 (2000) 613.
[24] Y. Ishii, Catal. Today 117 (1–3) (2006) 105.
[25] Y. Ishii, S. Sakaguchi, T. Iwahama, Adv. Synth. Catal. 343 (5) (2001) 393.
[26] R.A. Sheldon, I.W.C.E. Arends, Adv. Synth. Catal. 346 (9–10) (2004) 1051.
[27] R.A. Sheldon, I.W.C.E. Arends, J. Mol. Catal. A Chem. 251 (1–2) (2006) 200.
[28] F. Minisci, C. Punta, F. Recupero, F. Fontana, G.F. Pedulli, J. Org. Chem. 67 (8) (2002) 2671.
[29] R. Amorati, M. Lucarini, V. Mugnaini, G.F. Pedulli, F. Minisci, F. Recupero, F. Fontana, P. Astolfi, L. Greci, J. Org. Chem. 68 (5) (2003) 1747.
[30] F. Minisci, F. Recupero, G.F. Pedulli, M. Lucarini, J. Mol. Catal. A Chem. 204 (2003) 63.
[31] F. Minisci, F. Recupero, A. Cecchetto, C. Gambarotti, C. Punta, R. Faletti, R. Paganelli, G.F. Pedulli, Eur. J. Org. Chem. 1 (2004) 109.
[32] I. Hermans, L. Vereecken, P.A. Jacobs, J. Peeters, Chem. Commun. 9 (2004) 1140.
[33] I. Hermans, P. Jacobs, J. Peeters, Phys. Chem. Chem. Phys. 9 (6) (2007) 686.
[34] S. Koguchi, K. Tomoya, Tetrahedron Lett. 47 (2006) 2797.

[35] F. Cozzi, Adv. Synth. Catal. 348 (2006) 1367.
[36] F. Rajabi, J.H. Clark, B. Karimi, D.J. Macquarrie, Org. Biomol. Chem. 3 (2005) 725.
[37] O. Anton, P. Jacobs, G. Poncelet, P. Jacques, Eur. Patent 0 159 578, 1985, to Redco N.V.
[38] I. Hermans, P.A. Jacobs, J. Peeters, Chem. Phys. Chem. 7 (2006) 1142.